Available online at www.sciencedirect.com

SciVerse ScienceDirect

Ceramics International 38 (2012) 1859–1866

CERAMICS INTERNATIONAL

www.elsevier.com/locate/ceramint

Nano-structured CuO films prepared by simple solution methods: Plate-like, needle-like and network-like architectures

F. Bayansal *, H.A. Çetinkara, S. Kahraman, H.M. Çakmak, H.S. Güder

Physics Department, Mustafa Kemal University, 31034 Hatay, Turkey

Received 6 September 2011; received in revised form 3 October 2011; accepted 4 October 2011
Available online 8 October 2011

Abstract

Two simple, safe and environmental friendly chemical solution methods which are suitable to mass production, applicable at low temperatures and cost effective, were used to prepare homogenous nano-structured cupric oxide (CuO) films. By using different types of substrates (glass, quartz, Cu foil and Si) and techniques various types of CuO nanostructures (plate, needle and network like) were produced. The products were characterized by scanning electron microscopy, X-ray diffraction and temperature dependant dark electrical resistivity measurements in order to investigate the effects of substrate on morphology, crystallographic structure and electrical properties of the films. From these characterizations it was seen that there are significant differences in the morphological, crystallographic, structural and electrical properties of the nanostructures that were produced by different techniques and/or on different substrates. Besides, growth mechanisms of CuO films have been investigated.

Keywords: Nanostructure; CuO; Electrical resistivity/conductivity; Band gap energy; Substrate effect; Thin film

1. Introduction

Nano-structured materials such as nanotubes [1,2], nanowires [3–6], nanorods [7–9], nanoribbons [10,11] and nanosheets [12–14] have attracted more attention in the last decades due to their unique optical, electrical and magnetic properties and their potential applications in nanodevices [15]. Nano-materials exhibit outstanding and surprising properties with the decrease in the dimensions and the change in shape and in crystal structure. Because of these unique and predictable properties, they can be used in nano-scaled electronic devices. Owing to these novel properties, many researchers work on nano-structured materials in order to use them as building blocks for the integration of the next generation of nanoelectronics, ultra small optical devices, gas sensors, biosensors and so on.

In recent years, cupric oxide (CuO) has attracted increasing interest for its prospective applications in many fields. As an important low cost and non-toxic transition metal oxide with a narrow bandgap of ~1.2 eV at room temperature, copper oxide films have received much attention for its various applications some of which are in catalysis [16], semiconductors [17], batteries [18], gas sensors [19], biosensors [20], magnetic storage media [21], solar cells [22], electronics [23], varistors [24], capacitors [25] and field transistors [26]. Because the chemical and physical properties of CuO are strictly dependant of its morphology, in recent years considerable efforts have been made to synthesize various types of CuO nanostructures. A number of different techniques such as heating copper sheets in O_2 atmosphere [6], immersing CuO sheets into ammonia or sodium hydroxide solutions [27], electrodepositing Cu(II) ions [28] or using a wet-chemical route [29] have been used to control size and morphology of CuO nanomaterials. Among these techniques, chemical bath deposition method (CBD) – a wet-chemical method – and direct reaction with ammonia or sodium hydroxide solutions are promising techniques because they are both simple, safe, environmental friendly, suitable to mass production, low temperature and cost effective solution methods. By using these different methods, considerable powder samples of CuO nanoparticles have been reported [30,31]. But nano-structured CuO thin films that were grown on a substrate have been reported seldomly. In some of them, Cu foils were used [27,32], but only in a few of them some other materials like microscope glasses and stainless steel slices

* Corresponding author. Tel.: +90 326 2455845; fax: +90 326 2455867.
E-mail address: fbayy@hotmail.com (F. Bayansal).

0272-8842/$36.00
doi:10.1016/j.ceramint.2011.10.011

[33,34] were used as substrates. For this reason, substrate effect on CuO films needs more investigations.

In this work we report a simple route for the synthesis of dense, continuous and stable nano-structured CuO films by two methods. The first method is immersing glass, quartz, silicon and Cu foil substrates in an aqueous solution of copper(II) chloride dehydrate and ammonia. And the other method is immersing Cu foils in an aqueous solution of ammonia and sodium hydroxide. The morphology of CuO nanostructures can be changed by using different types of substrates. We have investigated the growth mechanism, crystal structure and morphology of synthesized CuO films. Besides, we have investigated the temperature dependent dark electrical resistivity measurements in order to calculate the ionization energy values of the impurity levels and the band gap energy values of the films.

2. Experimental details

2.1. Materials

All the chemical reagents used in the experiment were analytical grade and were used without further purification. Copper(II) chloride dehydrate ($CuCl_2{\cdot}2H_2O$), sodium hydroxide (NaOH), sulfuric acid (H_2SO_4) and copper foil (Cu) were purchased from Sigma–Aldrich Co. Ammonia solution (NH_3) and acetone (CH_3COCH_3) were purchased from Merck KGaA. p-type Si wafers (boron doped, resistivity: 1–10 Ωcm, thickness: 400 μm) were purchased from Si-Mat.

2.2. Synthesis of CuO films on glass, quartz, Si and Cu substrates by CBD method

Synthesis of the films onto the glass, quartz, Si and Cu substrates were described as follows: at first, substrates were cleaned in three steps which are cleaning in dilute sulfuric acid solution (H_2SO_4:H_2O, 1:5, v/v), in absolute acetone and in de-ionized water (18.2 MΩ cm^{-2}) for 5 min each in an ultrasonic bath. Then, 1.705 g copper(II) chloride dehydrate ($CuCl_2{\cdot}2H_2O$) was dissolved in 100 ml de-ionized water under stirring in a magnetic stirrer at room temperature to obtain 0.1 M copper chloride solution. The solution was stirred for 1 h to ensure that $CuCl_2$ dissolved completely. Then, pH value of the solution was increased to ∼10.0 by adding aqueous ammonia (NH_3) under constant stirring. A blue solution of $Cu(OH)_2$ was soon produced. The pH of the solution was measured by Hanna pH 211/213 pH-meter. Previously cleaned glass, quartz, Si and Cu substrates were immersed into the solution. Glass substrates were tilted against the wall of beaker where the angle between the substrates and the beaker bottom is ∼60°. The other substrates were attached to a piece of glass and immersed into the solution as tilted where all of the substrates (quartz, Cu, polished and unpolished sides of Si) were positioned upward. Then the solution was started to boil at ∼90 °C in order to convert $Cu(OH)_2$ into CuO. Heating rate was 10 °C/min and it took about 10 min to boil the solution. After 15 min boiling, the substrates were taken out from the bath and rinsed in de-ionized water for about 5 min in an ultrasonic bath in order to remove larger and loosely bonded CuO particles. Before the analyses, the substrates were dried in air at room temperature for a day.

2.3. Synthesis of CuO films on Cu foils by solution method

Synthesis of the films onto Cu foils was described as follows: At first, copper foils (2 cm × 2 cm) were sandpapered and then washed in dilute sulfuric acid solution (H_2SO_4:H_2O, 1:5, v/v) for 5 min and subsequently washed with de-ionized water and absolute ethanol to remove the surface impurities as well as oxide layers. Next, a solution with pH ∼ 12.0 was prepared by adding enough amount of NaOH into 175 ml de-ionized water. Next, 15 ml NH_3 was added to the prepared solution. Then, the treated Cu foils were immersed into the above solution and kept at 80 °C for 48 h. Then, the solution cooled down to room temperature and the Cu foils kept at the solution for 48 h more. Finally, the Cu foils were taken out from the solution, washed with de-ionized water and dried at room temperature for a day. It was seen that the Cu foils were completely covered by black films (CuO films). After drying, one of the foils was annealed at 300 °C for 1 h in a PROTHERM PTF 12/50/450 tube furnace in order to investigate the heat treatment effect on the nano-scaled CuO structures. In our previous paper it was seen that heat treatment did not make more changes on the nano-structures that were grown glass substrates by CBD method [35].

2.4. Characterization of the samples

The crystal structure of the samples was examined by Philips X'pert Pro X-ray diffractometer (XRD) (CuKα radiation, λ = 1.540056 Å). A scan rate of 0.02°/s was applied to record the pattern in the 2θ range of 20–60°. A JEOL JSM-5500LV scanning electron microscope (SEM) was operated at an acceleration voltage of 20 kV for morphological imaging. Thickness values of some of the films were calculated by gravimetric methods and measured by crossectional SEM analyses. A Keithley 6487 Picoammeter/Voltage Source was used to investigate the temperature dependant dark electrical resistivity measurements in order to calculate the ionization energy values of impurity levels and the band gap energy values of the films.

3. Results and discussion

3.1. Morphology

Morphology and microstructure of the CuO films were investigated by SEM. As seen from the Fig. 1, CuO plates form CuO clusters on the glass substrates. Fig. 1(a) shows the SEM image of the back side of a glass substrate (the surface which having the angle of 60° with the beaker surface) where formation of CuO clusters was very week. On the other hand, on the front side of the glass substrates (Fig. 1(b)), all of the CuO clusters touch to each other and form continuous films that are necessary for electrical conductivity. Fig. 2 shows the SEM images of front sides of as-synthesized and annealed (at 300 °C for 1 h) CuO films. It can be seen that the substrates are fully

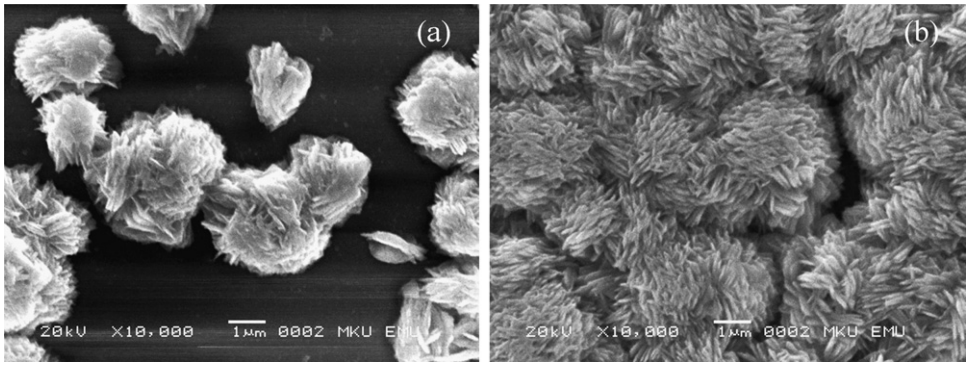

Fig. 1. SEM images of (a) back side and (b) front side of the glass substrate.

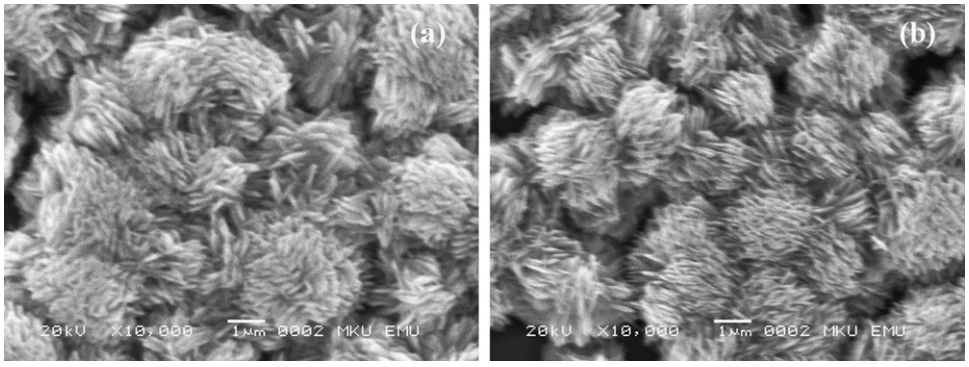

Fig. 2. SEM images of front sides of the CuO nanoplates: (a) as-synthesized and (b) annealed at 300 °C for 1 h.

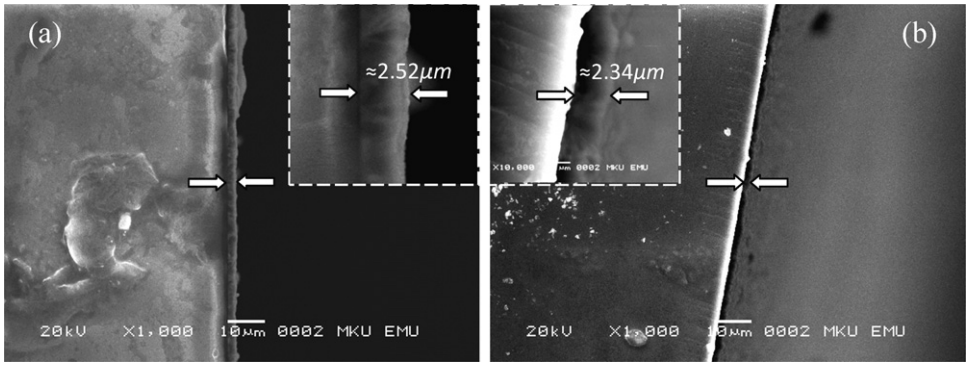

Fig. 3. Cross sectional SEM images of front sides of the CuO films: (a) as-synthesized and (b) annealed at 300 °C for 1 h.

covered by clusters of CuO nanoplates. Annealing process decreases both the diameter of clusters and thickness of nanoplates. Before annealing the average cluster diameter is ∼2.5 μm and the average thickness of the nanoplates is ∼110 nm. After annealing the average cluster diameter decreases to ∼1.9 μm and the average nanoplate thickness decreases to 75 nm. Fig. 3 shows the cross-sectional SEM images of front sides of as-synthesized and annealed films. Average thickness of front sides of as-synthesized films is 2.5 μm; on the other hand the average thickness of annealed films is 2.3 μm. These values are listed in Table 1. From the gravimetric measurements the average film thickness (front

Table 1
Band gap energy and impurity level ionization energy values, cluster diameters, film and nanoplate/wire thickness values and nanowire lengths of the samples.

Substrates	E_g (eV)	ΔE (eV)	Cluster diameter (μm)	Film thickness (μm)	Plate/wire thickness (nm)	Wire length (μm)
Glass (as-synthesized)	1.37	0.30	2.5 ± 0.5	2.5 ± 0.2	110 ± 20	–
Glass (annealed)	1.39	0.32	1.9 ± 0.6	2.3 ± 0.2	75 ± 25	–
Cu foil (solution method)	1.47	0.42	2.1 ± 0.8	2.6 ± 0.2	87 ± 10	–
Cu foil (CBD method)	1.45	0.40	–	–	80 ± 10	–
Quartz	1.40	0.39	–	–	95 ± 11	1.0 ± 0.4
Silicon	1.40	0.38	–	–	84 ± 12	0.8 ± 0.3

side) was found as about 1.9 μm for as-synthesized films which implies that the porosity (≈24%) of the films is high. Also the decrease in the front side thickness of the annealed film that measured by gravimetric method is in accordance with that of the crossectional SEM measurements. Heat treatment can cause a re-crystallization and can convert $Cu(OH)_2$ into CuO and H_2O. Re-crystallization or removing water from the structure may have caused a decrease in the sizes of the nanostructures, clusters and in the thickness of the films.

On the other hand if the substrates are crystalline, CuO nanostructures do not form clusters but they homogenously cover the whole surface of the crystalline substrate or they form clusters very close to each other that there seems no boundary between them as in Fig. 4. As seen from the images needle-like CuO nanostructures were grown on the substrates. The number of active bonding or adsorption centers on crystalline surfaces is higher than that is on non-crystalline or amorphous surfaces. In the case of high periodicity of atoms more active bonding or adsorption centers can occur on the surface. But in non-crystalline or amorphous surfaces week periodicity of atoms on the surface cause a decrease in the number of active bonding or adsorption centers. Average thickness values of the needle-like nanostructures are 95, 84 and 86 nm and the average lengths of these structures are 1.0, 0.8 and 0.9 μm, respectively for quartz (Fig. 4(a)), polished side of Si (Fig. 4(b)) and non-polished side of Si (Fig. 4(c)) substrates. In Fig. 4, it is also seen that there exists some CuO clusters on the surface. But these clusters were formed on the surfaces that were covered by CuO needles. And on non-polished side of the Si surface (Fig. 4(c)) it was seen that there were some sunk regions, this may be because of non-smooth surface.

Morphology of CuO particles on Cu foils are considerably different from that were grown on glass, quartz and Si substrates. Fig. 5 shows the SEM images of CuO nanoparticles that were grown on Cu foils. They were prepared by immersing Cu foils in ammonia and sodium hydroxide solution (Fig. 5(a) and (b)) and in copper chloride solution (Fig. 5(c)). In Fig. 5(a) and (b) it is seen that dense spherical CuO clusters were grown in network-like CuO nanowires. Fig. 5(b) shows the annealed CuO film while Fig. 5(a) shows as-synthesized CuO film. There exist some small changes in the sizes of the structures. In as-synthesized case average cluster diameter is 2.1 μm while in annealed case that is 2.6 μm. Addition of copper(II) chloride to the bath and/or different cleaning processes cause a sharp modification in the shape of CuO structures (Fig. 5(c)). By adding some new chemical to the solution can possibly cause some extra chemical reactions in the intermediate steps which could considerably affect the morphology of the films. In this case, plate-like structures were formed on the Cu surface as they were formed on the glass substrates. But instead of forming spherical CuO clusters, CuO nanostructures have been accumulated along some lines on the surface of Cu foils. In the cleaning process of the solution method, Cu foils were sandpapered and is expected to be rougher than that for CBD method. The different roughness could also impact the CuO morphology. The average thickness of CuO nanoplates is 80 nm. At least 10 different points chosen randomly from the different parts of the samples used for the evaluation of the average thickness, diameter and length values for each sample.

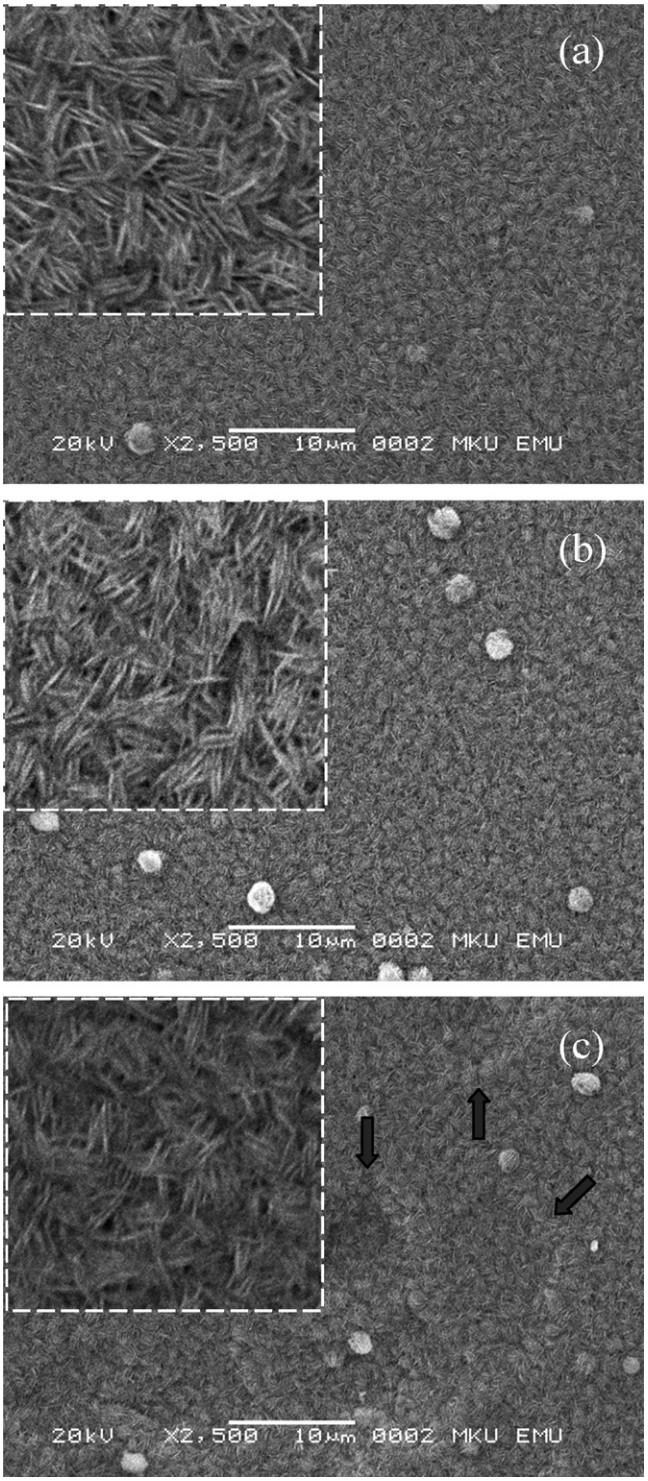

Fig. 4. SEM images of the needle-like CuO nanostructures that were deposited on (a) quartz, (b) polished side of silicon and (c) non-polished side of silicon.

3.2. Crystal structure

XRD analyses were employed to study the crystal structures of the CuO films. Fig. 6 show typical XRD patterns of the as-synthesized and annealed (at 300 °C for 1 h) films that were

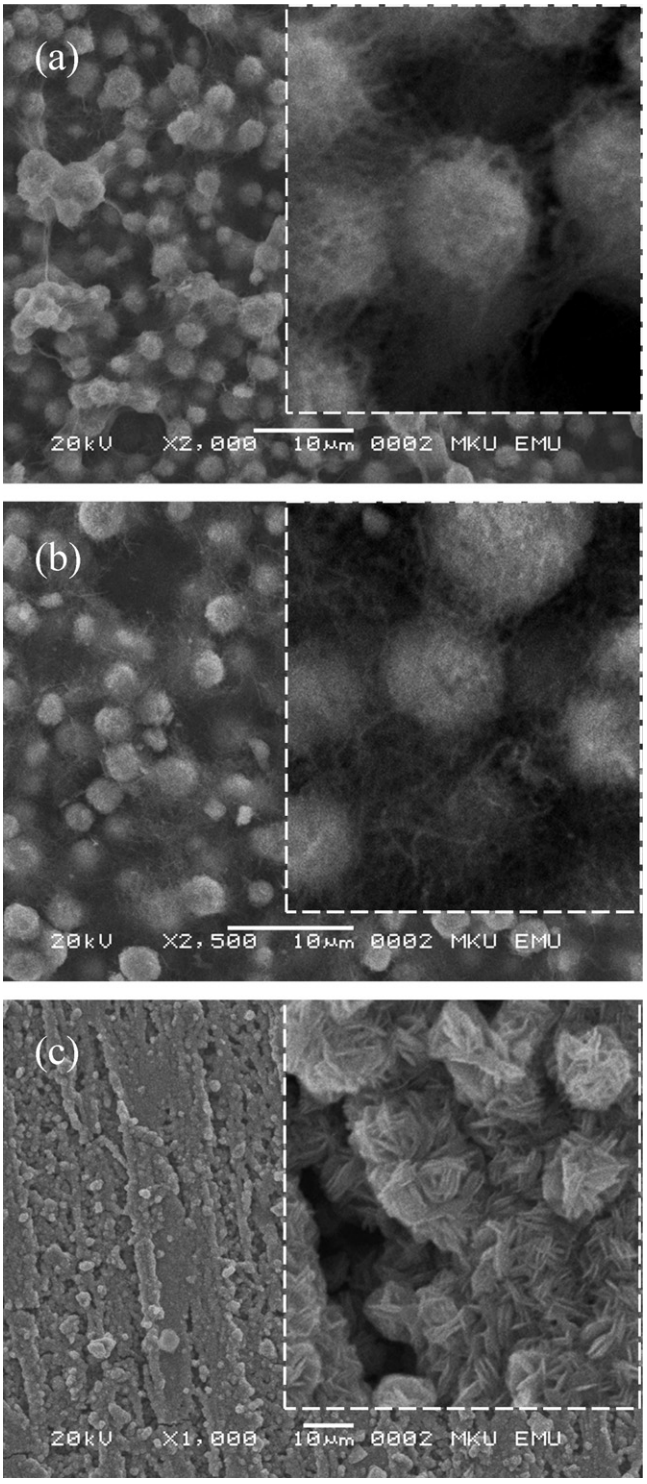

Fig. 5. SEM images of the network-like CuO nanostructures: (a) as-synthesized, (b) annealed and (c) plate-like CuO nanostructures on Cu foils.

grown on glass substrates. There were no XRD peaks referred to $Cu(OH)_2$, which means the grown film completely consist of only CuO molecules or $Cu(OH)_2$ may be present in small extent and accumulated along the grain boundaries of the crystallites constituting the film or $Cu(OH)_2$ may be amorphous [36]. XRD pattern also provides information on crystal orientations: the Miller-indexed $(0\,0\,2)/(\bar{1}\,1\,1)$ and $(1\,1\,1)/(2\,0\,0)$ reflections are

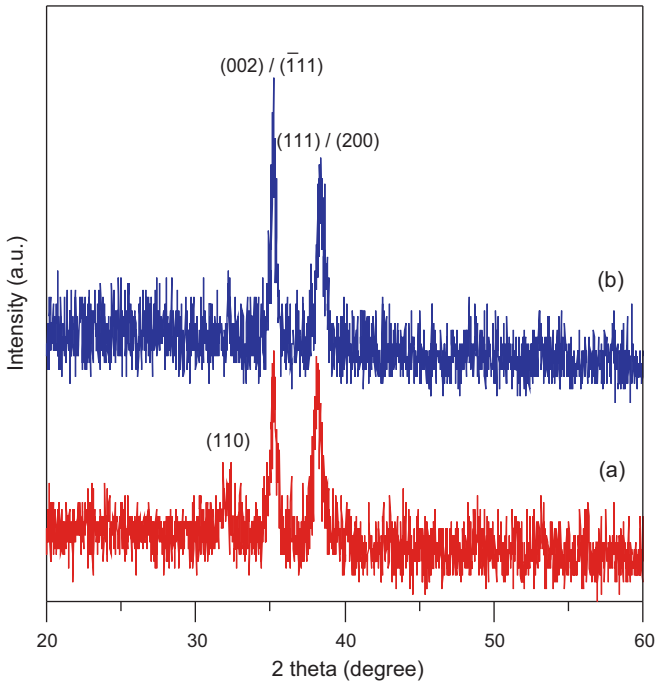

Fig. 6. XRD patterns of front sides of the CuO nanoplates: (a) as-synthesized and (b) annealed at 300 °C for 1 h.

the strongest, which indicate that they are preferential crystal planes of the nanoplates. From the XRD patterns it can be deduced that annealing causes an increase in the intensities of the peaks $(0\,0\,2)/(\bar{1}\,1\,1)$ and $(1\,1\,1)/(2\,0\,0)$ and causes a decrease in the intensity of $(1\,1\,0)$ peak. Intensity values of the peaks at $(0\,0\,2)/(\bar{1}\,1\,1)$ and $(1\,1\,1)/(2\,0\,0)$ orientations change from 38 to 49 and from 37 to 44, respectively. Fig. 7 shows the XRD patterns of the films that were grown on quartz and silicon substrates. From the figure it can be seen that the intensity values are not high as much as that are in Fig. 6 which means that formation of CuO nanostructures on glass substrates are stronger than that are on quartz and silicon substrates. But in this case there appears a peak shift towards higher 2θ values on both $(0\,0\,2)/(\bar{1}\,1\,1)$ and $(1\,1\,1)/(2\,0\,0)$ peaks. This fact indicates the presence of the lattice strains in the films. Fig. 8 shows the XRD patterns of the films that were grown on copper foils. Before annealing (Fig. 8(a)) $(0\,0\,2)/(\bar{1}\,1\,1)$ peak is dominant but after annealing (Fig. 8(b)) the intensity of this peak decreases and $(1\,1\,1)/(2\,0\,0)$ and $(\bar{2}\,0\,2)$ peaks appear. Fig. 8(c) shows the XRD pattern of CuO nanostructures that were grown on Cu foils in copper chloride bath. Interestingly, these three peaks have relatively lower intensities. All diffraction peaks for all samples can be clearly indexed to the monoclinic CuO phase with lattice constants of $a = 4.6797$ Å, $b = 3.4314$ Å, $c = 5.1362$ Å, and $\beta = 99.2620°$ (JCPDS Card No.: 01-080-0076).

3.3. Electrical measurements

Silver paste was used to make ohmic contacts with CuO thin films. *I–V* dependence of the films is linear within the studied voltage range which proves that the contacts are ohmic. The

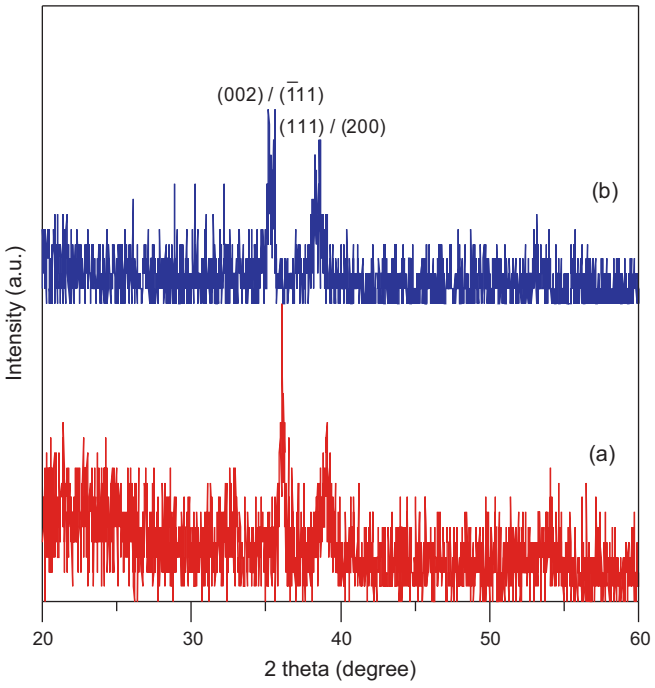

Fig. 7. XRD patterns of the needle-like CuO nanostructures that were grown on (a) quartz and (b) polished side of silicon substrates.

derivative $(\partial I/\partial V)^{-1}$ is constant and equal to the electrical resistance of investigated CuO thin film, indicating a negligible value of the contact resistance. We have measured the temperature dependence (in the range of 300 K–500 K) of dark electrical resistivity for all CuO films in order to determine the ionization energy values of the impurity levels and the thermal band gap energy values of the films. The details of the

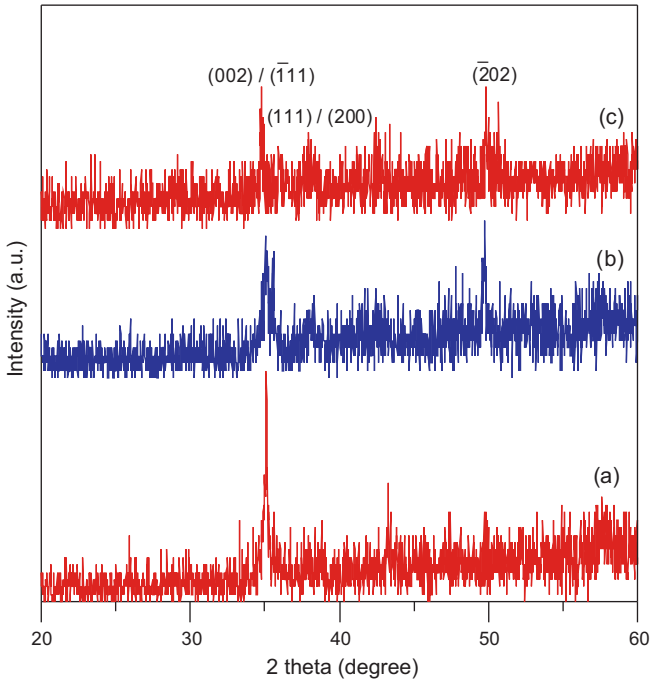

Fig. 8. XRD patterns of the network-like CuO nanostructures: (a) as-synthesized, (b) annealed and (c) plate-like CuO nanostructures on Cu foils.

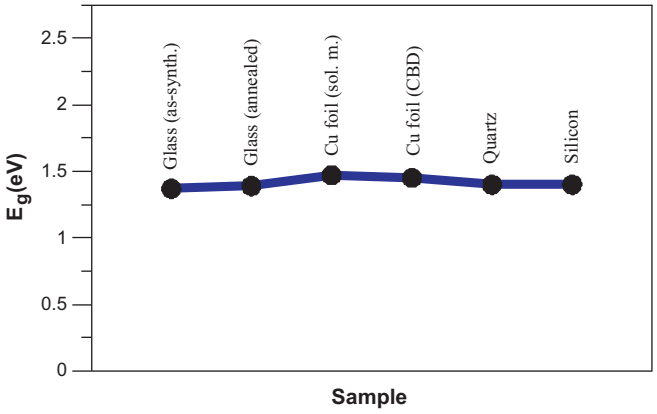

Fig. 9. Band gap energy values of the samples.

calculations are given in the previous work [35].

$$E_g = 2k\frac{d\ln(R(T))}{d(1/T)} \tag{1}$$

The band gap energies were calculated from the slopes of $\ln(R)$ vs. $1000/T$ graphs by using Eq. (1). The obtained E_g values of the samples (Fig. 9) are listed in Table 1. These values are in good agreement with the one obtained from optical spectroscopy measurements [29].

As seen from Fig. 10, there exists only one impurity level (one linear region at low temperatures).

$$\Delta E = k\frac{d\ln(R(T))}{d(1/T)} \tag{2}$$

The impurity level ionization energy values were calculated from the slopes of $\ln(R)$ vs. $1000/T$ graphs by using Eq. (2). The obtained impurity level ionization energy (ΔE) values of the samples (Fig. 11) are listed in Table 1.

3.4. The growth mechanism

For copper ions aqueous solution, when the ion product (IP) of the solution is higher than the solubility product (SP) the

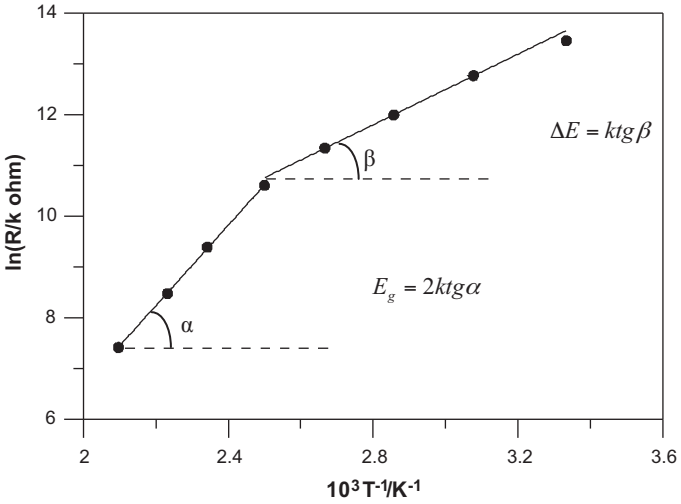

Fig. 10. $\ln R$ vs. $1/T$ dependence of the as-synthesized CuO films (front side).

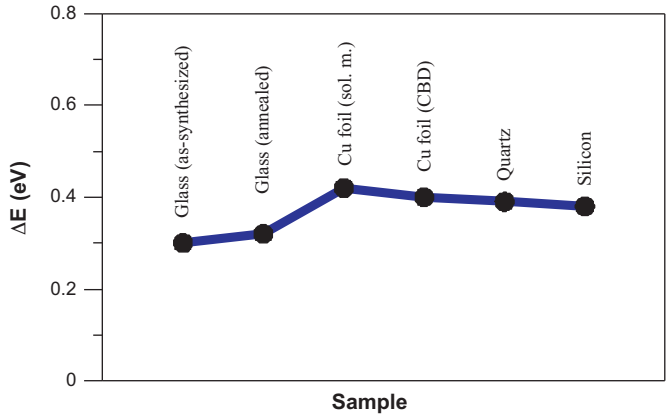

Fig. 11. Impurity level ionization energy values of the samples.

precipitation $Cu(OH)_2$ occurs. It is commonly accepted that the degree of supersaturation (S), defined as the ratio of IP to SP, is an important parameter to evaluate the precipitation process in aqueous solution. If S is lower than 1, no precipitation occurs. If S is higher than 1 but lower than a critical value S_c, a heterogeneous precipitation occurs on the walls of container and substrate because the value of S is not sufficient to induce nuclei in the bulk solution. And if S is higher than S_c, a homogenous precipitation occurs in the bulk solution [37]. According to this theory, S value for copper ions must be fixed in between 1 and S_c in order to get heterogeneous nucleation on the substrate.

In the first part of these series of experiments $CuCl_2{\cdot}2H_2O$ and NH_3 were used as ion source and reagent respectively. Cu^{2+} ions were obtained by dissolving 1.705 g $CuCl_2{\cdot}2H_2O$ in double distilled water as shown in Eq. (3). Before the start of precipitation reaction, the pH value of the solution was ~3.80. The possible chemical reactions are as follows:

$$CuCl_2{\cdot}2H_2O \rightarrow Cu^{2+}{}_{(aq)} + 2Cl^{-}{}_{(aq)} \quad (3)$$

$$NH_3 + H_2O \leftrightarrow NH_4{}^{+}{}_{(aq)} + OH^{-}{}_{(aq)} \quad (4)$$

$$NaOH + H_2O \rightarrow Na^{+}{}_{(aq)} + OH^{-}{}_{(aq)} \quad (5)$$

$$Cu^{2+}{}_{(aq)} + 2OH^{-}{}_{(aq)} \rightarrow Cu(OH)_2 \quad (6)$$

$$Cu(OH)_2 \rightarrow CuO + H_2O \quad (7)$$

In the suggested reaction scheme, ammonia played key role for the formation of desired CuO nanostructures. The pH value of the solution is raised to the value of ~10.0 by adding ammonia which introduces ammonium and OH? ions (Eq. (4)). This is the critical stage in the chemical reaction because this stage controls the supply of OH? ions which determines the degree of supersaturation S. And also $Cu(OH)_2$ precipitate cannot dissolve in the solution with a high OH? concentration to form dissoluble complex ions such as $Cu(OH)_4{}^{-2}$. Therefore we believe that CuO crystalline nuclei in nanoscale were formed in the dehydration of $Cu(OH)_2$ precipitate and gradually grown on the substrates and wall of the container. Subsequent heating of the solution (Eq. (7)) causes this decomposition. From the XRD patterns of the films that were synthesized in the copper(II) chloride solutions, it was concluded that the grown film were completely composed of only CuO molecules. In the second part NH_3 and NaOH played key role. Adding these two chemicals into the bath introduced OH? ions (Eqs. (4) and (5)). These OH? ions in the bath form $Cu(OH)_2$ by bonding to Cu atoms in the surface of Cu foil. We believe that subsequent heating of the solution (Eq. (7)) causes dehydration of $Cu(OH)_2$ into CuO.

4. Conclusion

In summary, we have synthesized dense, continuous and stable CuO films with good crystallinity in a short time, e.g. 15 min. SEM, XRD and temperature dependant dark electrical resistivity investigations on the nanostructures have been carried out. From SEM images, average thickness of the CuO nanostructures (plate, needle and wire) deposited on glass, quartz, silicon and copper substrates are found as ~100 nm. The XRD measurements showed that the CuO nanostructures have a high crystal quality with monoclinic crystal structure preferentially in (1 1 0), $(0\,0\,2)/(\bar{1}\,1\,1)$, (1 1 1)/(2 0 0) and $(\bar{2}\,0\,2)$ directions. From the temperature dependent dark electrical resistivity measurements, ionization energy values of the impurity levels have been calculated in between 0.30 and 0.42 eV and the band gap energy values have been calculated in between 1.37 and 1.47 eV.

Acknowledgements

This work is financially supported by Scientific Research Commission of Mustafa Kemal University (Project No: 1001M 0115).

References

[1] X. Wang, F. Zhang, B. Xia, X. Zhu, J. Chen, S. Qiu, P. Zhang, J. Li, Controlled modification of multi-walled carbon nanotubes with CuO, Cu_2O and Cu nanoparticles, Solid State Sciences 11 (2009) 655.
[2] M. Bockrath, W. Liang, D. Bozovic, J.H. Hafner, C.M. Lieber, M. Tinkham, H. Park, Resonant electron scattering by defects in single-walled carbon nanotubes, Science 291 (2001) 283.
[3] S.A. Meenach, J. Burdick, A. Kunwar, J. Wang, Metal/conducting-polymer composite nanowires, Small 3 (2007) 239.
[4] C.-Y. Huang, A. Chatterjee, S.B. Liu, S.Y. Wu, C.-L. Cheng, Photoluminescence properties of a single tapered CuO nanowire, Applied Surface Science 256 (2010) 3688.
[5] Y.-k. Su, C.-m. Shen, H.-t. Yang, H.-l. Li, H.-j. Gao, Controlled synthesis of highly ordered CuO nanowire arrays by template-based sol–gel route, Transactions of Nonferrous Metals Society of China 17 (2007) 783.
[6] X.Y. Fan, Z.G. Wu, P.X. Yan, B.S. Geng, H.J. Li, C. Li, P.J. Zhang, Fabrication of well-ordered CuO nanowire arrays by direct oxidation of sputter-deposited Cu_3N film, Materials Letters 62 (2008) 1805.
[7] M.H. Cao, C.W. Hu, Y.H. Wang, Y.H. Guo, C.X. Guo, E.B. Wang, A controllable synthetic route to Cu, Cu_2O, and CuO nanotubes and nanorods, Chemical Communications 15 (2003) 1884.
[8] S. Anandan, X. Wen, S. Yang, Room temperature growth of CuO nanorod arrays on copper and their application as a cathode in dye-sensitized solar cells, Materials Chemistry and Physics 93 (2005) 35.
[9] Y. Zeng, T. Zhang, M. Yuan, M. Kang, G. Lu, R. Wang, H. Fan, Y. He, H. Yang, Growth and selective acetone detection based on ZnO nanorod arrays, Sensors and Actuators B 143 (2009) 93.

[10] P. Gao, Y. Chen, H. Lv, X. Li, Y. Wang, Q. Zhang, Synthesis of CuO nanoribbon arrays with noticeable electrochemical hydrogen storage ability by a simple precursor dehydration route at lower temperature, International Journal of Hydrogen Energy 34 (2009) 3065.
[11] Q. Yu, M. Wang, H. Chen, Fabrication of ordered TiO_2 nanoribbon arrays by electrospinning, Materials Letters 64 (2010) 428.
[12] G. Wang, J. Huang, S. Chen, Y. Gao, D. Cao, Preparation and supercapacitance of CuO nanosheet arrays grown on nickel foam, Journal of Power Sources 196 (2011) 5756.
[13] J.G. Zhao, S.J. Liu, S.H. Yang, S.G. Yang, Hydrothermal synthesis and ferromagnetism of CuO nanosheets, Applied Surface Science 257 (2011) 9678.
[14] L. Zheng, X. Liu, Solution-phase synthesis of CuO hierarchical nanosheets at near-neutral pH and near-room temperature, Materials Letters 61 (2007) 2222.
[15] F. Favier, E.C. Walter, M.P. Zach, T. Benter, R.M. Penner, Hydrogen sensors and switches from electrodeposited palladium mesowire arrays, Science 293 (2001) 2227.
[16] T. Ishihara, M. Higuchi, T. Takagi, M. Ito, H. Nishiguchi, T. Takita, Preparation of CuO thin films on porous $BaTiO_3$ by self-assembled multibilayer film formation and application as a CO_2 sensor, Journal of Materials Chemistry 8 (1998) 2037.
[17] M. Singhai, V. Chhabra, P. Kang, D.O. Shah, Synthesis of ZnO nanoparticles for varistor application using Zn-substituted aerosol ot microemulsion, Materials Research Bulletin 32 (1997) 239.
[18] L.B. Chen, N. Lu, C.M. Xu, H.C. Yu, T.H. Wang, Electrochemical performance of polycrystalline CuO nanowires as anode material for Li ion batteries, Electrochimica Acta 54 (2009) 4198.
[19] P. Poizot, S. Laruelle, S. Grugeon, L. Dupont, J.M. Tarascon, Nano-sized transition-metal oxides as negative-electrode materials for lithium-ion batteries, Nature 407 (2000) 496.
[20] G.L. Luque, M.C. Rodriguez, G.A. Rivas, Glucose biosensors based on the immobilization of copper oxide and glucose oxidase within a carbon paste matrix, Talanta 66 (2005) 467.
[21] R.V. Kumar, Y. Diamant, A. Gedanken, Sonochemical synthesis and characterization of nanometer-size transition metal oxides from metal acetates, Chemistry of Materials 12 (2000) 2301.
[22] H. Cao, S.L. Suib, Highly efficient heterogeneous photooxidation of 2-propanol to acetone with amorphous manganese oxide catalysts, Journal of the American Chemical Society 116 (1994) 5334.
[23] R. Ao, L. Kümmerl, D. Haarer, Present limits of data storage using dye molecules in solid matrices, Advanced Materials 7 (1995) 495.
[24] Y. Jiang, S. Decker, C. Mohs, K.J. Klabunde, Catalytic solid state reactions on the surface of nanoscale metal oxide particles, Journal of Catalysis 180 (1998) 24.
[25] H. Zhang, M. Zhang, Synthesis of CuO nanocrystalline and their application as electrode materials for capacitors, Materials Chemistry and Physics 108 (2008) 184.
[26] W. Jia, E. Reitz, P. Shimpi, E.G. Rodriguez, P.X. Gao, Y. Lei, Spherical CuO synthesized by a simple hydrothermal reaction: concentration-dependent size and its electrocatalytic application, Materials Research Bulletin 44 (2009) 1681.
[27] W. Zhang, S. Ding, Z. Yang, A. Liu, Y. Qian, S. Tang, S. Yang, Growth of novel nanostructured copper oxide (CuO) films on copper foil, Journal of Crystal Growth 291 (2006) 479.
[28] S. Wei, Y. Chen, Y. Ma, Z. Shao, Fabrication of CuO/ZnO composite films with cathodic co-electrodeposition and their photocatalytic performance, Journal of Molecular Catalysis A: Chemical 331 (2010) 112.
[29] R.A. Zarate, F. Hevia, S. Fuentes, V.M. Fuenzalida, A. Zuniga, Novel route to synthesize CuO nanoplatelets, Journal of Solid State Chemistry 180 (2007) 1464.
[30] N.R.E. Radwan, M.S. El-Shall, H.M.A. Hassan, Synthesis and characterization of nanoparticle Co_3O_4, CuO and NiO catalysts prepared by physical and chemical methods to minimize air pollution, Applied Catalysis A: General 331 (2007) 8.
[31] C.L. Carnes, K.J. Klabunde, The catalytic methanol synthesis over nanoparticle metal oxide catalysts, Journal of Molecular Catalysis A: Chemical 194 (2003) 227.
[32] S.C. Vanithakumari, S.L. Shinde, K.K. Nanda, Controlled synthesis of CuO nanostructures on Cu foil, rod and grid, Materials Science and Engineering B 176 (2011) 669.
[33] H.T. Hsueh, T.J. Hsueh, S.J. Chang, F.Y. Hung, T.Y. Tsai, W.Y. Weng, C.L. Hsu, B.T. Dai, CuO nanowire-based humidity sensors prepared on glass substrate, Sensors and Actuators B 156 (2011) 906.
[34] Y. Xu, C. Wang, D. Chen, X. Jiao, Fabrication and characterization of novel nanostructured copper oxide films via a facile solution route, Materials Letters 64 (2010) 249.
[35] F. Bayansal, S. Kahraman, G. Çankaya, H.A. Çetinkara, H.S. Güder, H.M. Çakmak, Growth of homogenous CuO nano-structured thin films by a simple solution method, Journal of Alloys and Compounds 509 (2011) 2094.
[36] V.R. Shinde, C.D. Lokhande, R.S. Mane, S.H. Han, Hydrophobic and textured ZnO films deposited by chemical bath deposition: annealing effect, Applied Surface Science 245 (2005) 407.
[37] G. Hodes, Chemical Solution Deposition of Semiconductor Films, Marcel Dekker, Inc., New York, 2002, 377 p.